SONIC BOOM INTERACTION WITH TURBULENCE

Zvi Rusak and Thomas E. Giddings
Department of Mechanical Engineering, Aeronautical Engineering and Mechanics
Rensselaer Polytechnic Institute, Troy, New York 12180-3590

A recently develped transonic small-disturbance model is used to analyze the interactions of random disturbances with a weak shock. The model equation has an extended form of the classic small-disturbance equation for unsteady transonic aerodynamics. It shows that diffraction effects, nonlinear steepening effects, focusing and caustic effects and random induced vorticity fluctuations interact simultaneously to determine the development of the shock wave in space and time and the pressure field behind it. A finite-difference algorithm to solve the mixed-type elliptic hyperbolic flows around the shock wave is presented. Numerical calculations of shock wave interactions with various deterministic vorticity and temperature disturbances result in complicate shock wave structures and describe peaked as well as rounded pressure signatures behind the shock front, as were recorded in experiments of sonic booms running through atmospheric turbulence.

INTRODUCTION

The review of various experimental and theoretical investigations of the interaction of shock waves and specifically sonic booms with free stream vortical or turbulent flows shows (Rusak and Cole[1]) that this complex nonlinear interaction is still an open problem. Specifically, the improved simulation of sonic boom propagation through the real atmosphere requires a better understanding of the interaction of weak shocks with vortical perturbations and turbulence.

Analysis of experimental data and theoretical approaches shows that in the case of the sonic boom, the shock waves near the ground are very weak, but still stronger than any acoustic wave. Also, flow fluctuations due to the atmospheric turbulence or vortical shear flows can become comparable to the shock weak strength such that locally the shock strength can be either strongly reduced or magnified and the shock wave front can be distorted significantly. Therefore, linearized acoustics and its second-order scattering

problem, or first-order linear theories of shock-vorticity interaction do not represent correctly the development of the weak shock and the pressure field behind it. However, in a coordinate system moving with the basic weak shock, the problem may fit the transonic framework.

In a recent paper, Rusak and Cole[1] have presented a new extended transonic small-disturbance model to describe the interactions of random fluctuations with a weak shock wave. The model equation also has an extended form of the classic nonlinear acoustics equation that describes the propagation of sound beams with narrow angular spectrum (KKZ equation)[2-3] and is similar to the model equation of Pierce[4]. The model shows that diffraction effects, nonlinear steepening effects, focusing and caustic effects and random induced vorticity fluctuations interact simultaneously to determine the development of the shock wave in space and time and the pressure field behind it.

This paper summarizes the theory of Rusak and Cole[1]. A finite-difference algorithm to solve the mixed-type elliptic hyperbolic flows around the shock wave is also presented. Numerical calculations of weak shock wave interactions with deterministic vorticity and temperature disturbances describe both peaked or rounded pressure signatures as were recorded in experiments of sonic booms running through atmospheric turbulence[5-10].

A TRANSONIC SMALL DISTURBANCE MODEL

The analysis of the linearized problem of the interaction of a weak shock with small disturbances shows[1] that it is an invalid approach when the flow perturbations are of the order of the shock strength. Therefore, a different approach has been developed to study the interaction of weak shocks with comparable random fluctuations in the flow (Rusak and Cole)[1]. In a coordinate system moving with a basic given weak shock, the problem may fit the framework of transonic theory. A transonic small-disturbance model has been developed to analyze the flow across a basic weak shock running in the (−x) direction. A coordinate system attached to the basic shock is considered. The velocity vector ($\underset{\sim}{V}$), pressure (P), density ($\bar{\rho}$) and vorticity ($\underset{\sim}{\omega}$) are described every where in the flow by:

$$
\begin{aligned}
\underset{\sim}{V} &= U_\infty \Big\{ \underset{\sim}{i}\,(1 + \epsilon^{2/3}\,u + \epsilon u_1 + \epsilon^{4/3}\,u_2 + \cdots) \\
&\qquad + \underset{\sim}{j}\,(\epsilon v_1 + \epsilon^{4/3}\,v_2 + \cdots) + \underset{\sim}{k}\,(\epsilon w_1 + \epsilon^{4/3}\,w_2 + \cdots)\Big\} \\
P &= p_\infty\,(1 + \epsilon^{2/3} p + \epsilon p_1 + \epsilon^{4/3}\,p_2 + \cdots) \\
\bar{\rho} &= \rho_\infty\,(1 + \epsilon^{2/3}\rho + \epsilon\rho_1 + \epsilon^{4/3}\,\rho_2 + \cdots) \\
\underset{\sim}{\omega} &= \epsilon^{2/3}(\underset{\sim}{j}\omega_y + \underset{\sim}{k}\omega_z) + \epsilon\,(\underset{\sim}{i}\omega_{x1} + \underset{\sim}{j}\omega_{y1} + \underset{\sim}{k}\omega_{z1}) + \cdots
\end{aligned}
\tag{1}
$$

where $U_\infty = a_\infty(1 + K/2\ \epsilon^{2/3})$ is the speed of the basic shock ($K > 0$) and a_∞, p_∞, ρ_∞ are the speed of sound, pressure and density of the unperturbed flow ahead of the shock. ($\epsilon^{2/3}$) represents the scale of strength of the basic weak shock where $\epsilon << 1$. A rescaling of the x-coordinate and time (t) has also been considered: $x^* = x/\epsilon^{1/3}$ and $t^* = ta_\infty\,\epsilon^{1/3}$, such that each of the terms in (1) is a function of (x^*, y, z, t^*). The rescaling in x means a stretching of the picture of the flow around the basic shock in order to capture the basic nonlinear effects that occur in the flow across the shock. The rescaling in time accounts for low-frequency unsteady perturbations in the flow. The constant K reflects that the speed of the basic shock wave is slightly higher than the speed of sound ahead of the shock. The substitution of Eqs. (1) into the continuity, momentum and energy equations results in (Rusak and Cole[1]):

$$u + \rho = f(y,z,t^*) \tag{2a}$$

$$\gamma u + p = g(y,z,t^*) \tag{2b}$$

$$-2\,\frac{\partial u}{\partial t^*} + \Big(-K - f + g - (\gamma+1)u\Big)\,\frac{\partial u}{\partial x^*} + \frac{\partial v_1}{\partial y} + \frac{\partial w_1}{\partial z} = -\frac{1}{\gamma}\,\frac{\partial g}{\partial t^*} \tag{2c}$$

$$\omega_y = \frac{\partial u}{\partial z} - \frac{\partial w_1}{\partial x^*} = \frac{1}{\gamma}\,\frac{\partial g}{\partial z} \tag{2d}$$

$$-\omega_z = \frac{\partial u}{\partial y} - \frac{\partial v_1}{\partial x^*} = \frac{1}{\gamma}\,\frac{\partial g}{\partial y} \tag{2e}$$

where f and g are random induced fluctuations due to the free turbulence. The function g is related to the vorticity fluctuations in the flow and the function f is due to temperature or speed of sound fluctuations. Equations (2) show that the axial perturbation (u), pressure perturbation (p) and density perturbation (ρ), that are of the order of the shock strength ($\epsilon^{2/3}$), interact with the transverse velocity perturbations v_1 and w_1, that are of a smaller scale (ϵ).

The substitution of $u = g/\gamma + \bar{u}$ in (2c), (2d) and (2e) results in a problem for solving a velocity potential function $\phi(x^*, y, z, t^*)$ where:

$$\bar{u} = \frac{\partial \phi}{\partial x^*}, \quad v_1 = \frac{\partial \phi}{\partial y}, \quad w_1 = \frac{\partial \phi}{\partial z}, \quad p = -\gamma \frac{\partial \phi}{\partial x^*} \tag{3a}$$

$$2\phi_{x^*t^*} + \left[K + \frac{g}{\gamma} + f + (\gamma + 1)\phi_{x^*}\right]\phi_{x^*x^*} - (\phi_{yy} + \phi_{zz}) = -\frac{1}{\gamma}\frac{\partial g}{\partial t^*}. \tag{3b}$$

In a conservative form Eq. (3b) is given by:

$$\left[2\,\phi_{x^*} + \frac{1}{\gamma} g\right]_{t^*} + \left[(K + g/\gamma + f)\,\phi_{x^*} + (\gamma + 1)\,\phi_{x^*}^2/2\right]_{x^*} - (\phi_y)_y - (\phi_z)_z = 0. \tag{3c}$$

The exact shock jump conditions (Ref. 11) must be satisfied along any shock surface $x^* - h(y, z, t^*) = 0$ that may appear in the solution. To the leading orders, they result in:

$$[f] = 0, \qquad [g] = 0, \tag{4a}$$

$$-2\left[\phi_{x^*}\right]\frac{\partial h}{\partial t^*} + \left(K + \frac{g}{\gamma} + f\right)\left[\phi_{x^*}\right] + (\gamma + 1)\left[\frac{\phi_{x^*}^2}{2}\right] + \left[\phi_y\right]\frac{\partial h}{\partial y} + \left[\phi_z\right]\frac{\partial h}{\partial z} = 0, \tag{4b}$$

$$\left[\phi_y\right] + \left[\phi_{x^*}\right]\frac{\partial h}{\partial y} = 0, \qquad \left[\phi_z\right] + \left[\phi_{x^*}\right]\frac{\partial h}{\partial z} = 0. \tag{4c}$$

where [a] represents the jump across the shock property a, $[a] = 7_B - a_A$. Equations (4a) show that to the leading order there is no jump in entropy across the shock, [S] = 0. Equations (1) and (2) also show that the local Mach number M_ℓ at any point in the flow is given by:

$$M_\ell^2 - 1 = \epsilon^{2/3}\, u^*, \qquad u^* = \left\{(\gamma+1)\,\phi_{x^*} + K + f + \frac{g}{\gamma}\right\}. \tag{5}$$

The flow is locally supersonic when $(\gamma+1)\,\phi_{x^*} + K + f + g/\gamma > 0$, sonic when $(\gamma+1)\,\phi_{x^*} + K + f + g/\gamma = 0$, and subsonic when $(\gamma+1)\,\phi_{x^*} + K + f + g/\gamma < 0$. Equations (3) and (4) are an extended version of the classic small-disturbance equation for unsteady transonic aerodynamics (Cole and Cook[12]). The changes are due to the random terms g and f. Starting from given functions for f and g and initial conditions that describe a given basic shock, Eqs. (3) and (4) can be integrated in space and time to describe the development of the shock wave and pressure field behind it.

An alternative approach has also been found by taking an x*-derivative of (2c) and using Eq. (2a). The pressure perturbation (p) satisfies the equation:

$$\frac{\partial}{\partial x^*}\left[\frac{\partial p}{\partial t^*} + \frac{K + f + g/\gamma}{2} - \frac{\gamma+1}{2\gamma}\, p\, \frac{\partial p}{\partial x^*}\right] = \frac{1}{2}\left[\frac{\partial^2 p}{\partial y^2} + \frac{\partial^2 p}{\partial z^2}\right]. \tag{6}$$

Equation (6) is an extended version of the classic KKZ equation that describes the propagation of nonlinear sound beams with narrow angular spectrum in an inviscid fluid (Zabolotskaya et al.[2], Kuznetsov[3]). Equation (6) also has a similar form to the model equation that has been recently developed by Pierce[4] using logical considerations only.

Equations (3) and (6) show that diffraction effects, nonlinear steepening, focusing and caustic effects, and random induced fluctuations due to turbulence interact simultaneously to determine the development of the shock wave in space and time and the pressure field behind it. Turbulence tends to change the local speed of sound in the flow across the shock and through this effect to reduce or to magnify the strength of the jump along the basic shock (see Eq. (5)) or to distort the shock front. These changes may result in unsteady motion of the shock front or in caustic vertices or in reflected shocks behind the incident wave that can produce the variety of pressure signatures of sonic booms that are measured in experiments[5-10].

FINITE DIFFERENCE SCHEME

A finite difference algorithm to solve the unsteady mixed-type elliptic-hyperbolic flow around the shock wave has been developed. Murman and Cole[13] and Cole and Cook[12] techniques are used. A fully conservative scheme that is based on the conservative form of Eq. (3c) is derived. In this way the difference equations also contain the shock relations (Eqs. (4)).

Consider a uniform finite difference mesh (Δx^*, Δy, Δz, Δt^*) in space and time, with points (x^*, y, z, t^*) labeled by (i, j, k, n). The results can be easily generalized to a variable mesh. Equation (3c) can be expressed in a conservative flux form for a box centered on a mesh point (i, j, k). Therefore,

$$\frac{1}{\Delta t^*}\left\{\left(2\phi_{x^*}+\frac{1}{\gamma}g\right)_{(i,j,k,n)}-\left(2\phi_{x^*}+\frac{1}{\gamma}g\right)_{(i,j,k,n-1)}\right\}$$

$$+\frac{1}{\Delta x^*}\left\{\left(\left(K+\frac{1}{\gamma}g+f\right)\phi_{x^*}+(\gamma+1)\,\phi_{x^*}^2/2\right)_{(i+1/2,j,k,n)}\right.$$

$$\left.-\left(\left(K+\frac{1}{\gamma}g+f\right)\phi_{x^*}+(\gamma+1)\,\phi_{x^*}^2/2\right)_{(i-1/2,j,k,n)}\right\}$$

$$-\frac{1}{\Delta y}\left\{(\Phi_y)_{(i,j+1/2,k,n)}-(\phi_y)_{(i,j-1/2,k,n)}\right\}$$

$$-\frac{1}{\Delta z}\left\{(\Phi_z)_{(i,j,k+1/2,n)}-(\phi_z)_{(i,j,k-1/2,n)}\right\}=0. \qquad (7)$$

In Eq. (7), (ϕ_y) and (ϕ_z) are always calculated from a centered expression. However, the approximation of (ϕ_{x^*}) strongly depends on whether locally, at a point, the flow is subsonic, supersonic, sonic or if it is a shock point. Extending References 12 and 13 methodologies to our case and using Eq. (5), a centered approximation and a backward expression are given for u^*:

$$u^{*c}_{(i,j,k,n)} = K + f(j,k,n) + \frac{1}{\gamma} g(j,k,n)$$

$$+ \frac{\gamma+1}{2\Delta x^*} \left(\phi(i+1,j,k,n) - \phi(i-1,j,k,n) \right)$$

$$u^{*b}_{(i,j,k,n)} = K + f(j,k,n) + \frac{1}{\gamma} g(j,k,n)$$

$$+ \frac{\gamma+1}{2\Delta x^*} \left(\phi(i,j,k,n) - \phi(i-2,j,k,n) \right). \qquad (8)$$

The local type of the flow is determined by the following table:[12,13]

condition	u^{*c}	u^{*b}	local flow is
1	< 0	< 0	subsonic
2	> 0	> 0	supersonic
3	> 0	< 0	a sonic point
4	< 0	> 0	a shock point

Table 1. Algorithm for local type of flow

Equation (7) has been developed in a specific form according to the local type of the flow. The variety of difference forms for locally subsonic, supersonic, sonic or shock points are described in Rusak and Cole.[1]

Starting from initial conditions that describe a given shock wave in the space for $t = 0$ (or $n = 0$), and given temperature fluctuations $f(y,z,t)$ and vorticity perturbations $g(y,z,t)$, the various difference forms can be applied for $n = 1$ at any mesh point according to Table 1. They can be solved by an iterative point or line – or plane – relaxation algorithm until at any point max $|G(i,j,k,1)| < \delta$ where δ is a given small tolerance of convergence. Then $\phi_{x^*}(i,j,k,1)$ can be calculated at any mesh point and the process is restarted for the next time step. In this way the shock motion and pressure field behind it can be integrated in space and time and the effect of various deterministic and random fluctuations f and g can be studied.

NUMERICAL RESULTS

The finite difference algorithm to solve Eq. (3b) has been applied to a variety of two-dimensional and steady shock wave interactions with vorticity and temperature disturbances. Several problems have been studied where a nominal shock wave with $K = 1.2$ centered in the middle of the computational domain has been considered. The following boundary conditions were used: $\phi_{x^*} = 0$ along inlet surface, $\phi_{x^*} = -1.0$ along outlet surface (which satisfy the basic shock jump relations) and $\phi_{y^*} = 0$ along upper and lower surfaces.

The first case considered vorticity fluctuations only where $f = 0$ and

$$g(y) = \begin{cases} 0 & 0 \leq y \leq 1/4 \\ 0.5 \sin 4\pi(y - 1/4) & 1/4 \leq y \leq 3/4 \\ 0 & 3/4 \leq y \leq 1 \, . \end{cases} \tag{9}$$

Calculated pressure fields and profiles along various cross sections are shown in Figures 1 and 2. The bending of the shocks is in phase with the velocity perturbations (i.e., a positive velocity perturbation produces a downstream deflection and visa versa) as was also described by Ribner[14]. Relative to nominal shock conditions (Figure 2a), the pressure jump decreases noticeably (approximately 40%) where the shock is bent upstream (Figure 2b), and increases significantly (approximately 40%) where the shock is distorted downstream (Figure 2d). The rippled wavefront leads to focusing and defocusing effects behind the shock, where diffraction effects also become dominant.

In the second case only temperature disturbances have been considered where $g = 0$ and

$$f(y) = \begin{cases} 0 & 0 \leq y \leq 1/4 \\ 0.5 \sin 16\pi(y - 1/4) & 1/4 \leq y \leq 3/4 \\ 0 & 3/4 \leq y \leq 1 \, . \end{cases} \tag{10}$$

Pressure fields and profiles along cross sections are presented in Figures 3 and 4. Again, shock wave distortion results in significant local pressure jump reductions and increases

(see Figures 4b and c). Basic effects involved are similar to those described in the first case. Temperature or speed of sound disturbances strongly affect the basic shock as much as vorticity disturbances.

The third case combined shock wave interaction with both vorticity and temperature disturbances as are given by Eqs. (9) and (10), respectively. Calculated results are shown in Figures 5 and 6. The shock front distortion is more pronounced and composed of the basic two harmonics of the imposed disturbances. It is found that shock pressure jump at certain locations is nearly eliminated due to the combined effects, resulting in a rounded pressure profile (Figure 6b). At other locations along the shock front, the pressure jump is significantly increased relative to the nominal shock jump with approximately 70% (see Figure 6c).

CONCLUSIONS

A new transonic small-disturbance model has been developed where a rescaling of the axial coordinate and time has been considered to capture the basic nonlinear effects that occur in the flow across the shock. This model results in two alternative approaches: (1) an equation for solving a velocity potential function that is described by an extended version of the classic small-disturbance equation for unsteady transonic aerodynamics[12], and (2) a nonlinear stochastic equation to describe the pressure field that is similar to the model equation recently presented by Pierce[4] using logical considerations only. This equation also has an extended form of the classic equation that describes the propagation of nonlinear sound beams with narrow angular spectrum[2,3].

Both approaches show that diffraction effects, nonlinear steepening, focusing and caustic effects and random induced turbulence fluctuations interact simultaneously to determine the development of a shock wave in space and time and the pressure field behind it. Turbulence fluctuations tend to change the local speed of sound in the flow across the shock and through this effect to reduce or magnify the strength of the basic shock.

A finite difference scheme that uses Murman and Cole[13] finite-difference techniques for solving mixed-typed elliptic hyperbolic flows with shock waves has also been presented. Numerical simulations of two-dimensional and steady shock wave interactions with various deterministic vorticity and temperature disturbances have been shown. Results describe

C-2

complicate shock wave structures and peaks as well as rounded local pressure signatures behind the distorted shock fronts. Similar signatures were recorded in the experiments of sonic booms running through atmospheric turbulence[5-10].

ACKNOWLEDGEMENT

This work was carried out with the support of the NASA Langley Research Center under Award NAG-1-1362 and NASA Training Grant NGT-S1113. The authors would like to acknowledge Dr. G.L. McAninch for funding and monitoring this research.

REFERENCES

1. Rusak, Z. and Cole, J.D., "Interaction of the Sonic Boom with Atmospheric Turbulence," NASA CP 10132, May 1993, pp. 65-91. (Also: AIAA Paper 93-1943).

2. Zabolotskaya, E.A. and Khorkhlov, R.V., *Akust. Zhurnal* 15, 1, 1969, pp. 40.

3. Kuznetsov, V.O., *Akust. Zhurnal* 6, 4, 1970, pp. 548.

4. Pierce, A.D., "Wave Equations and Computational Models for Sonic Boom Propagation Through a Turbulent Atmosphere," NASA CP-3172, February 1992, pp. 31-48.

5. Hubbard, H.H., Maglieri, D.J., Huckel, V. and Hilton, D.A., "Ground Measurements of Sonic Boom Pressures for the Altitude Range of 10,000 to 75,000 Feet," NASA TR R-198, July 1964.

6. Maglieri, D.J., "Sonic Boom Flight Research – Some Effects of Airplane Operations and the Atmosphere on Sonic Boom Signatures," in *Sonic Boom Research,* Edited by Seebass, A.R., NASA SP-147, April 1967.

7. Garrick, I.E. and Maglieri, D.J., "A Summary of Results on Sonic Boom Pressure-Signature Variations Associated with Atmospheric Conditions," NASA TN D-4588, May 1968.

8. Downing, M.J., "Lateral Spread of Sonic Boom Measurements from U.S. Air Force Boomfile Flight Tests," NASA CP-3172, February 1992, pp 117-135.

9. Willshire, Jr., W.L. and Devilbiss, D.W., "Preliminary Results from the White Sands Missile Range Sonic Boom Propagation Experiments," NASA CP-3172, February 1992, pp. 137-149.

10. Lipkens, B. and Blackstock, T.T., "Model Experiment to Study the Effect of Turbulence on Risetime and Waveform of N Waves," NASA CP-3172, February 1992, pp. 97-107.

11. Courant, R. and Friedrichs, K.O., *Supersonic Flow and Shock Waves,* Interscience Publishers, Inc., New York, pp. 297-302, 1948.

12. Cole, J.D. and Cook, L.P., *Transonic Aerodynamics,* North-Holland, 1986.

13. Murman, E.M. and Cole, J.D., "Calculation of Plane Steady Transonic Flows," *AIAA Journal,* Vol. 9, pp. 114-121.

14. Ribner, H.S., "Cylindrical Sound Wave Generated by Shock-Vortex Interaction," *AIAA Journal,* Vol. 23, No. 11, 1985, pp. 1708-1715.

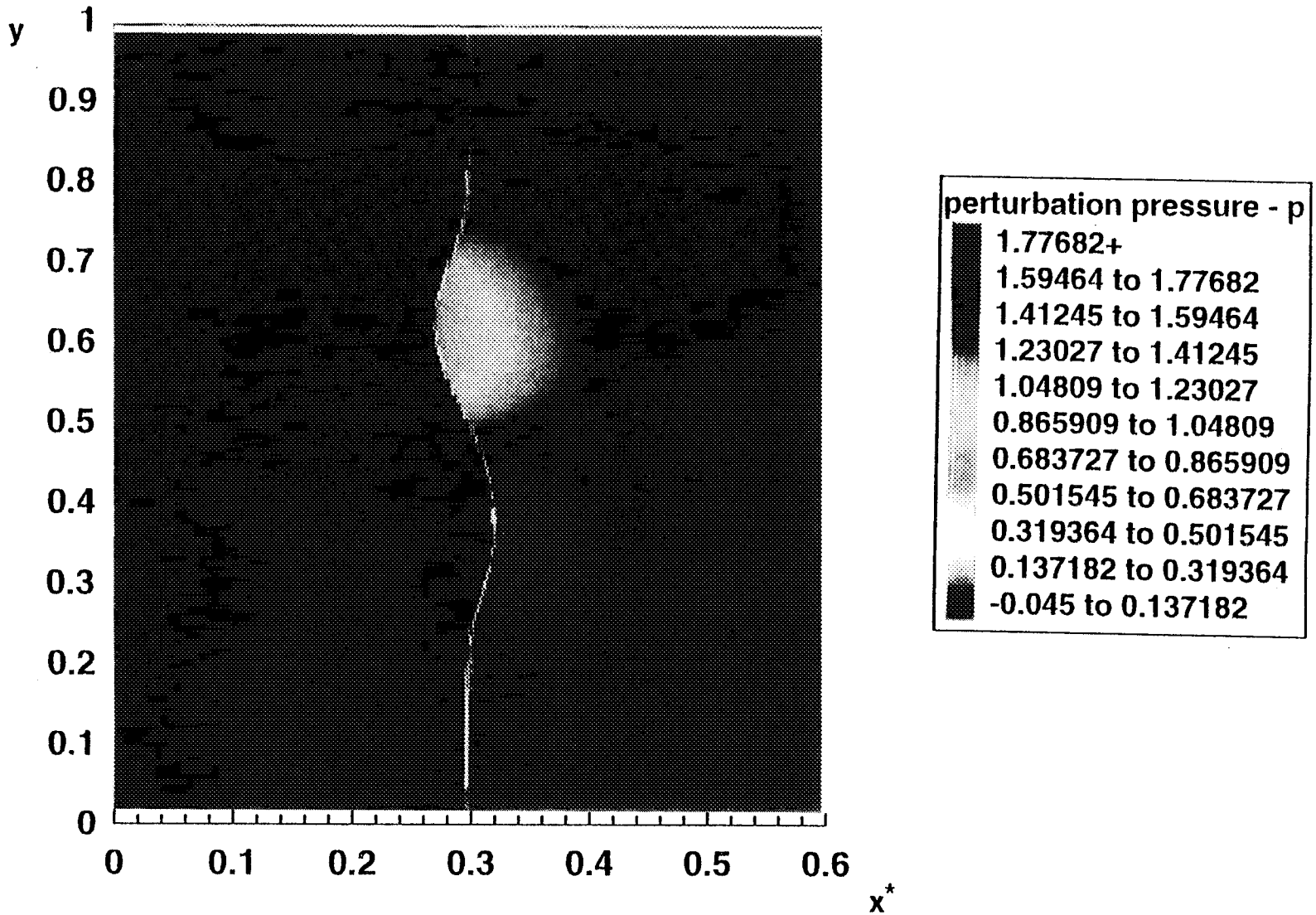

Figure 1. Pressure field for vorticity fluctuations (9).

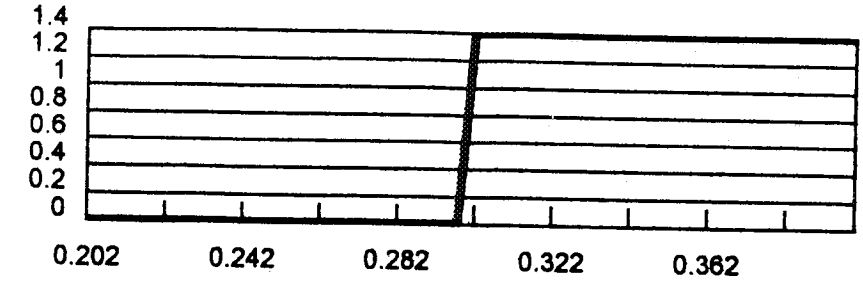

(a) y = 0.9 - Nominal Shock Wave Solution

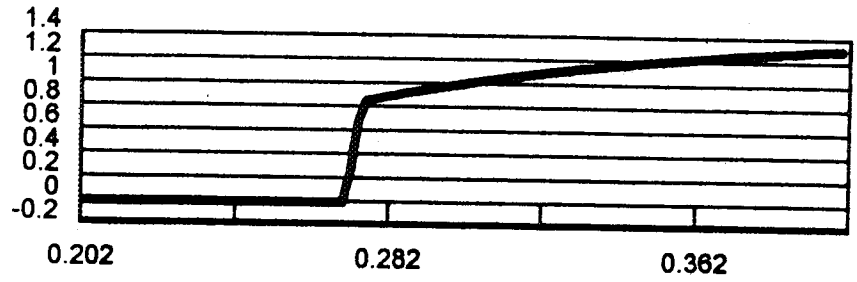

(b) y = 0.6

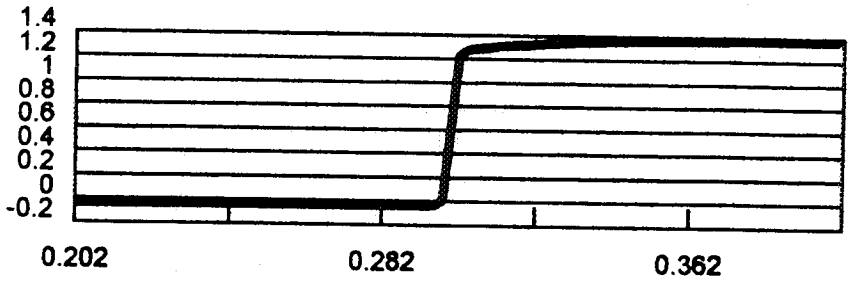

(c) y = 0.5

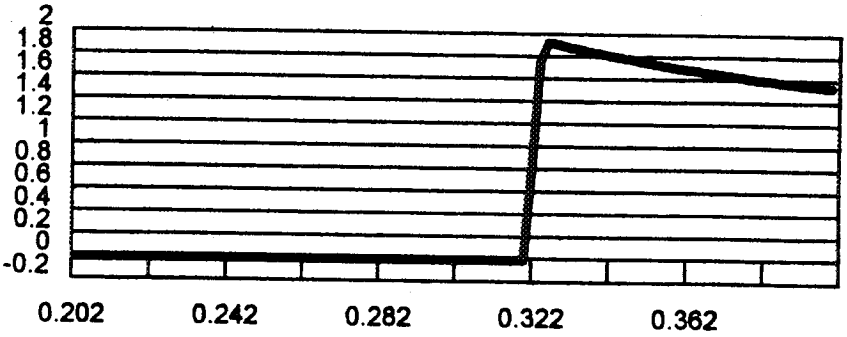

(d) y = 0.4

Figure 2. Pressure profiles along various cross sections for vorticity fluctuations (9).

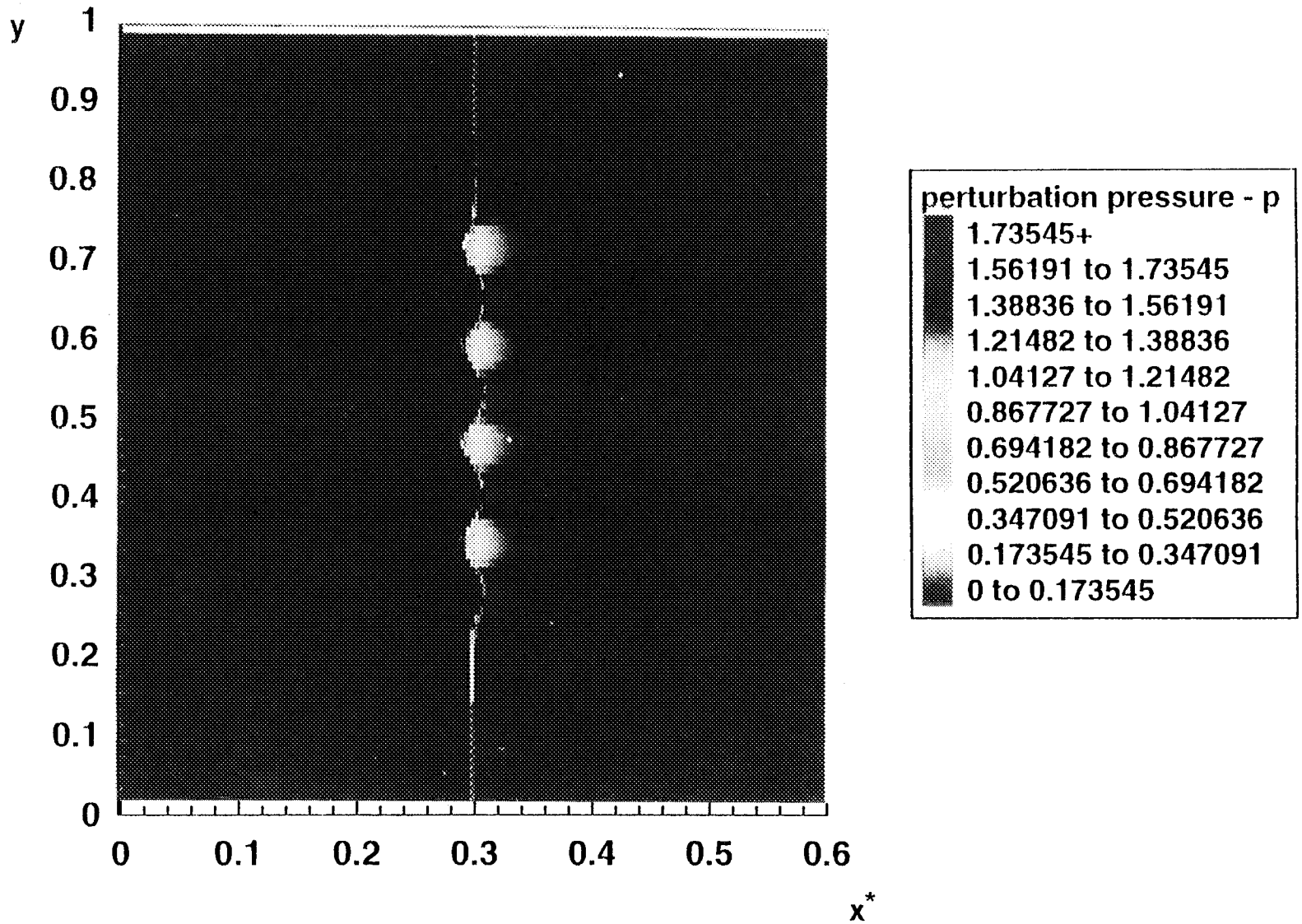

Figure 3. Pressure field for temperature disturbances (10).

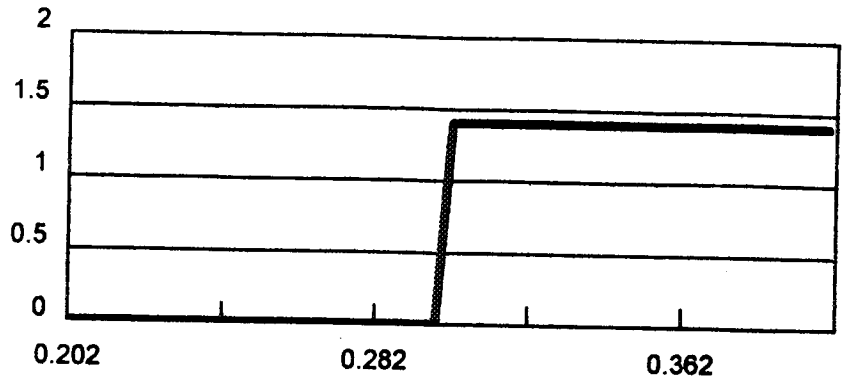

(a) y = 0.9 - Nominal Shock Wave Solution

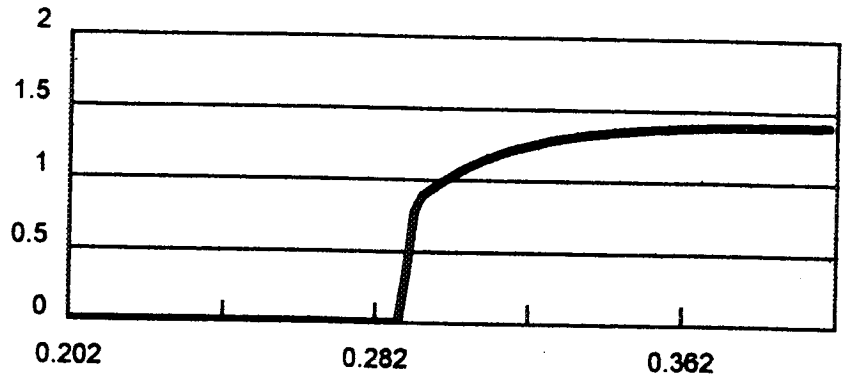

(b) y = 0.6

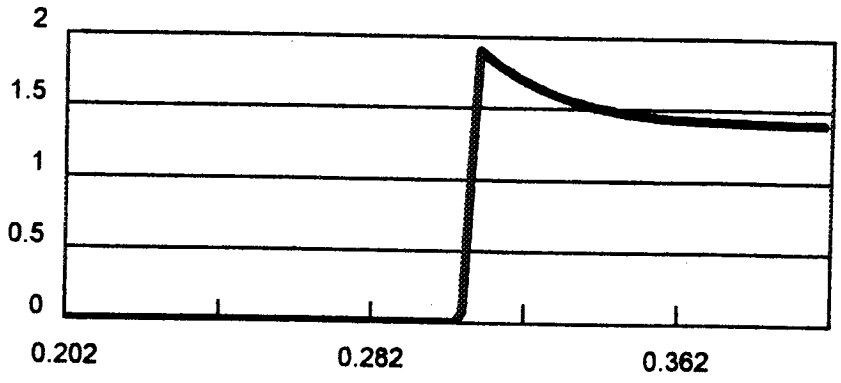

(c) y = 0.41

Figure 4. Pressure profiles along various cross sections for temperature disturbances (10).

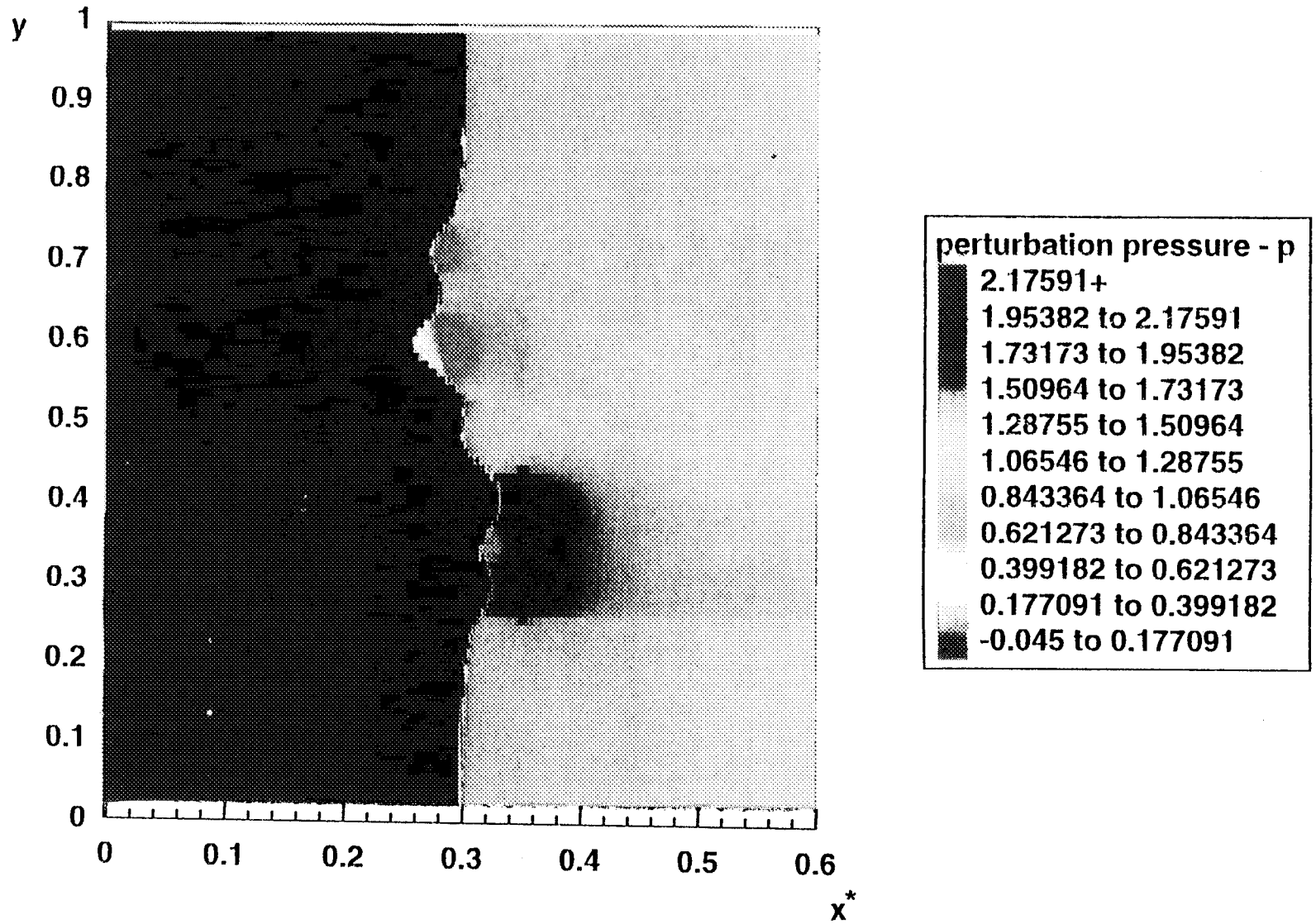

Figure 5. Pressure field for combined vorticity and temperature disturbances.

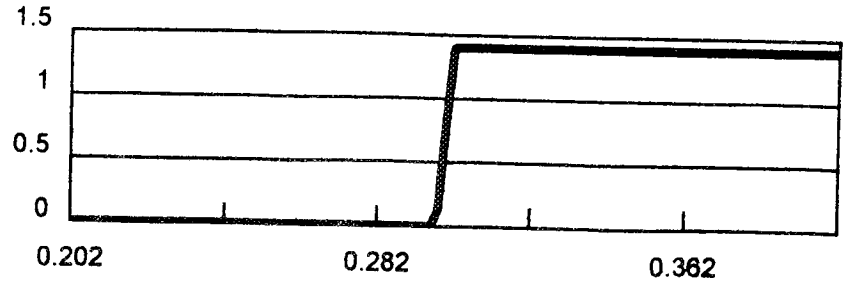

(a) y = 0.9 - Nominal Shock Wave Solution

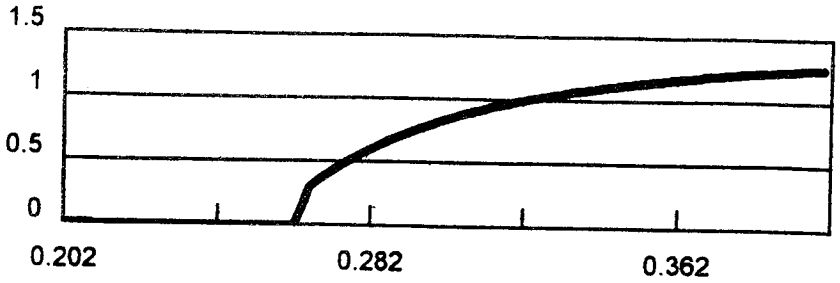

(b) y = 0.6

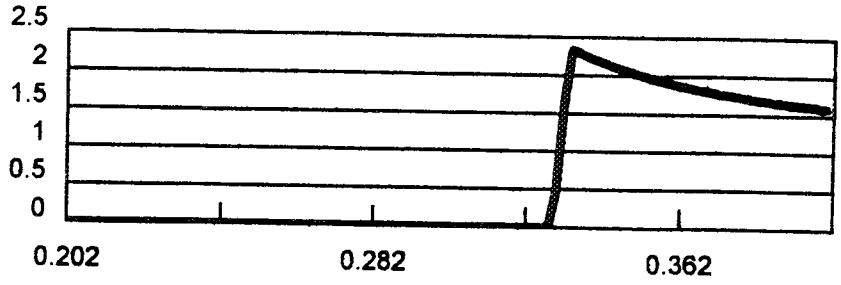

(c) y = 0.4

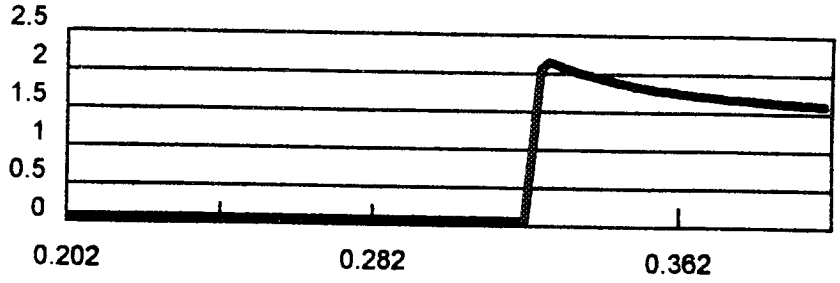

(d) y = 0.3

Figure 6. Pressure profiles along various cross sections for combined disturbances.